

A nonparametric Bayesian analysis of heterogeneous treatment effects in digital experimentation

Matt Taddy (taddy@chicagobooth.edu)
University of Chicago Booth School of Business

Matt Gardner
EBay

Liyun Chen
EBay

David Draper
University of California, Santa Cruz

Abstract: Randomized controlled trials play an important role in how internet companies predict the impact of policy decisions and product changes. Heterogeneity in treatment effects refers to the fact that, in such ‘digital experiments’, different units (people, devices, products) respond differently to the applied treatment. This article presents a fast and scalable Bayesian nonparametric analysis of heterogeneity and its measurement in relation to observable covariates. New results are provided for quantifying uncertainty about four different statistics that practitioners use to index heterogeneity: two based on linear projections and two based upon regression tree partitioning. For the linear projections, we mostly find that our Bayesian nonparametric inference agrees with results from the frequentist literature. For the regression trees, we are able to provide uncertainty quantification where this was previously difficult without restrictive assumptions. We survey the application of these statistics in three common tasks: recovery of the average treatment effect, sparse summarization of the linear projections, and partitioning into groups of relatively homogeneous response to treatment. Throughout, the work is illustrated with an example experiment involving 21 million unique users of EBay.com.

Taddy is also a scientific consultant at EBay and a Neubauer Family faculty fellow at the University of Chicago. The authors thank others at EBay who have contributed, especially Jay Weiler who assisted in data collection.

1 Introduction

The internet is host to a massive amount of experimentation. Online companies are constantly experimenting with changes to the ‘user’ experience. Randomized controlled trials are particularly common; they are referred to within technology companies as ‘A/B testing’ for the random assignment of control (option A) and treatment (option B) to experimental units (often users, but also products, auctions, or other dimensions).¹ The treatments applied can involve changes to choice of the advertisements a user sees, the flow of information to users, the algorithms applied in product promotion, the pricing scheme and market design, or any aspect of website look and function. EBay, the source of our example application, is constantly experimenting with these and other parts of the user experience, with the goal of making it easier for buyers and sellers of specific items to find each other.

Heterogeneous treatment effects (HTE) refer to the phenomenon wherein the treatment effect for any individual user – the difference between how they *would* have responded under treatment rather than control – is different from the average. It seems self-evident that HTE exist: different experimental units (people, products, or devices) will each have unique responses to treatment. The task of interest is to measure this heterogeneity. Suppose that for each user i with response y_i , in either control or treatment, $d_i = 0$ or $d_i = 1$ respectively, there are available some pre-experiment attributes, \mathbf{x}_i . These attributes might influence the effect of d_i on y_i . For example, if y_i is *during-experiment* user spend, then \mathbf{x}_i could include *pre-experiment* spend by user i on our website. We can then usefully index the HTE as a function of \mathbf{x}_i .

Today’s digital (i.e., internet) experiments differ from most prior experimentation in important ways. First, the sample sizes are enormous. Our example EBay experiment has a sample size of over 21 million unique users. Second, the effect sizes are tiny. Our example treatment – increasing the size of product images – has response standard deviation around 1000 times larger than the estimated treatment effect. Finally, the response of interest (some transaction, such as user clicks or money spent) tends to be distributed with a majority spike at zero, an extremely long tail, and residual variance that is correlated with available covariates. These data

¹This A/B terminology is common regardless of the number of treatment factors. The framework is widely used, even over-used: A/B testing is applied in many scenarios where significance testing for causal effects may not be the true goal, or where active learning, say via multi-armed bandits as in Scott (2010), would be more efficient.

features – large samples for learning complex structures, tiny effects that require careful uncertainty quantification, and strange distributions that defy summarization through a parametric model – provide a natural setting for nonparametric statistics. This article proposes a scalable framework for the Bayesian nonparametric analysis of heterogeneous treatment effects. Our main contribution is the application of this framework in a survey of four strategies for predicting HTE: based upon either linear or tree models, fit either to surrogates for the treatment effect on the full dataset or separately to the observed response within each treatment group.

Our approach to Bayesian nonparametric analysis is detailed in Section 3. There are two main steps: we define a flexible Bayesian model for the data generating process, say $g(d, \mathbf{x}, y)$, and derive from this the implied posterior distributions for target functionals of g . The remainder of the article is devoted to analysis of four potential techniques for indexing HTE on covariates. Section 4 details these statistics: two that define a linear projection of the treatment effect onto covariates, and two that correspond to regression trees which partition the covariate space into regions of relatively homogeneous treatment effect. Section 5 provides strategies for posterior inference, including analytic approximations for posterior moments of the linear projections. Given these main ingredients – the Bayesian model, the HTE statistics, and posterior inference strategies – we then work through a few common application areas. Section 6 describes inference for average treatment effects and compares strategies based on each of the four HTE statistics. Section 7 considers sparse summarization for the linear projection via a Bayesian decision theoretic framework. Section 8 studies the search for a stable partitioning rule based upon posterior variance of the regression trees. We close with a short discussion.

Throughout, we will reference large existing literatures on Bayesian parametric and semi-parametric analysis of HTE, which attempt to predict unobserved potential outcomes, and on frequentist analyses of HTE under different sampling models. We are not aiming to replace these existing frameworks, nor are we advocating for any one HTE statistic over another; indeed, it is impossible to judge their relative merits without positing some true value set or parametric form for the HTE. Instead, we simply present a survey of Bayesian nonparametric uncertainty quantification and summarization for these statistics. The hope is that frequentists and parametric Bayesians alike will benefit from this alternative point-of-view.

2 Data: notation and an illustrative example

For each experimental unit i , which we label a ‘user’ in analogy to our illustrative example, there is a response y_i , a binary treatment indicator d_i where $d_i = 0 \Rightarrow i \in c$ (in control) and $d_i = 1 \Rightarrow i \in t$ (in treatment), and a length $(p + 1)$ covariate vector $\mathbf{x}_i = [1, x_{i1}, \dots, x_{ip}]'$ (\mathbf{x}_{i0} is always an intercept).² There are n_c users in control, n_t in treatment, and $n = (n_c + n_t)$ in total. The $n_d \times (p + 1)$ designs for control and treatment groups are \mathbf{X}_c and \mathbf{X}_t , respectively, and these are accompanied by response vectors \mathbf{y}_c and \mathbf{y}_t . Stacked design and response are $\mathbf{X} = \begin{bmatrix} \mathbf{X}_c \\ \mathbf{X}_t \end{bmatrix}$ and $\mathbf{y} = \begin{bmatrix} \mathbf{y}_c \\ \mathbf{y}_t \end{bmatrix}$, so that $i = 1 \dots n_c$ are in control and $i = n_c + 1 \dots n$ are treated.

Our example experiment involves 21 million users of the website EBay.com, randomly assigned 2/3 in treatment and 1/3 in control over a five week period. The treatment of interest is a change in image size for items in a user’s ‘myEBay’ page – a dashboard that keeps track of items that the user has marked as interesting. In particular, the pictures are increased from 96 pixels in control to 140 pixels for the treated. The experiment is typical of a ‘product’ experiment at EBay, where we are exploring user response to small changes on the website.

2.1 User spend and other internet transaction data

At EBay, where buyers and sellers transact sales and purchases of items listed on the website, an important outcome variable is the per-buyer gross volume of merchandise bought: the total amount that a user *spends* on purchases during the experiment. This response is typical of internet transaction data, in that it has

- a majority at zero, since most users do not make a transaction during the experiment;
- an extremely long and fat right tail, corresponding to heavy spend by a minority of users;
- density spikes at, e.g., volumes linked to psychological price thresholds; and
- a variance that is correlated with both the treatment and sources of treatment heterogeneity. For our experiment, $\text{sd}(\mathbf{y}_t) = 1153$ is much higher than $\text{sd}(\mathbf{y}_c) = 970$.

²We assume this simple *single treatment factor* scenario for focus and ease of exposition, but it is straightforward to generalize our results to multi-factor treatment applications.

These characteristics make it practically impossible to devise parametric regression models. Even multi-stage linear models, say for $p(y > 0)$ and $\mathbb{E}[\log y \mid y > 0]$ as in Duan et al. (1983), are unbelievable here. Moreover, untransformed spending is the business-relevant response: for our results to be useful in decision making we need to understand treatment effects on the scale upon which EBay makes money.³ A nonparametric analysis is required.

2.2 Building covariates to index heterogeneity

Each covariate vector \mathbf{x}_i , representing potential sources of heterogeneity, is constructed from user behavior tracked before the beginning of the experiment. Most metrics are aggregated over the four weeks prior to the start of the experiment, but we also include longer-term information in a three-dimensional indicator for whether the user made any purchases in the past month, quarter, or year. The metrics tracked include

- transaction information such as total spending and number of bought items, sold items, or average price per bought item (treated as zero for zero bought items); and
- activity information such as counts for site-session visits, page or item views, and actions such as bidding on an item or asking a seller a question.

The variables are tracked in aggregate, as well as broken out by product category (e.g., collectibles, fashion, or ‘unknown’) and market platform (e.g., auction or fixed price).

This gives around 100 total raw variables; they are very sparse and highly correlated. For our tree models of Sections 4.3-4, these 100 covariates are input directly as continuous variables. For our linear models in Sections 4.1-2, the regression design is constructed by expanding each into indicators for whether the variable is greater than or equal to each of its *positive quintiles*. That is, there is a binary x_{ij} element to indicate when the corresponding raw covariate is greater than 0 and when it is greater than or equal to the 20th, 40th, 60th, and 80th percentile of nonzero sample values for that variable. After collapsing across equal quintiles (e.g., many variables have up to 60th nonzero percentile equal to one), this results in a 377 column design.

³For example, focusing on $p(y > 0)$ could drive the firm to target low-cost (and low-profit) items, and at the same time it is not difficult to define scenarios in which the mean effect is positive in $\log y$ but negative in y .

3 A Bayesian nonparametric model for the DGP

We employ Dirichlet-multinomial sampling as a flexible representation for the DGP. The approach dates back to Ferguson (1973), Chamberlain and Imbens (2003) overview it in the context of econometric problems, and Lancaster (2003) and Poirier (2011) provide detailed analysis of linear projections. Rubin (1981) proposed the Bayesian bootstrap as an algorithm for sampling from versions of the posterior implied by this strategy, and the algorithm has since become closely associated with this model.

This model represents the DGP through a probability mass function on a large but finite number of possible data points \mathbf{z} (including response, covariates, and treatment),

$$g(\mathbf{z}; \boldsymbol{\theta}) = \frac{1}{|\boldsymbol{\theta}|} \sum_{l=1}^L \theta_l \mathbb{1}[\mathbf{z} = \boldsymbol{\zeta}_l], \quad (1)$$

where $\mathcal{Z} = \{\boldsymbol{\zeta}_1 \dots \boldsymbol{\zeta}_L\}$ is the support of the DGP and $\boldsymbol{\theta}$ are random weights with $\theta_l \geq 0 \forall l$.⁴ Here $|\mathbf{v}|$ denotes $\sum_i |v_i|$, the L_1 norm. Observations are assumed drawn *independently* from (1) by first sampling l_i with probability θ_{l_i} and then assigning $\mathbf{z}_i = \boldsymbol{\zeta}_{l_i}$. A posterior over g is induced by the posterior over $\boldsymbol{\theta}$. Functionals of g , such as $\mathbb{E}_g f(\mathbf{z})$ for arbitrary function f and where \mathbb{E}_g implies expectation over $\mathbf{z} \sim g$, are thus random variables.

The conjugate prior for the normalized weight vector, $\boldsymbol{\theta}/|\boldsymbol{\theta}|$, is a Dirichlet distribution, written $\text{Dir}(\boldsymbol{\theta}/|\boldsymbol{\theta}|; \boldsymbol{\nu}) \propto \prod_{l=1}^L (\theta_l/|\boldsymbol{\theta}|)^{\nu_l-1}$. We specify a single concentration parameter $\boldsymbol{\nu} = a$, such that $\mathbb{E}[\theta_l/|\boldsymbol{\theta}|] = 1/L$ and $\text{var}(\theta_l/|\boldsymbol{\theta}|) = (L-1)/[L^2(La+1)]$. Suppose you have the observed sample $\mathbf{Z} = [\mathbf{z}_1 \dots \mathbf{z}_n]'$. For convenience, say each observation is unique⁵ and write $l_1 \dots l_n = 1 \dots n$ so that $\mathbf{z}_i = \boldsymbol{\zeta}_{l_i}$ and $\mathbf{Z} = [\boldsymbol{\zeta}_{l_1} \dots \boldsymbol{\zeta}_{l_n}]'$. Then the posterior distribution for $\boldsymbol{\theta}$ is $p(\boldsymbol{\theta}/|\boldsymbol{\theta}|) \propto \prod_{i=1}^n (\theta_{l_i}/|\boldsymbol{\theta}|)^a \prod_{l=n+1}^L (\theta_l/|\boldsymbol{\theta}|)^{a-1}$. The limiting prior that arises as $a \rightarrow 0$ is a default with massive computational convenience: in this limit, $\theta_l = 0$ with probability one for $l > n$.⁶ We apply this limiting prior throughout, such that our posterior for the data generating process is a multinomial draw from the *observed data points*. Overload notation and re-write

⁴We will often suppress $\boldsymbol{\theta}$ and write $g(\cdot)$ for $g(\cdot; \boldsymbol{\theta})$ unless the weights need to be made explicit.

⁵Or rather, we allow $\boldsymbol{\zeta}_l = \boldsymbol{\zeta}_k$ for $l \neq k$ in the case of repeated values.

⁶See Chamberlain and Imbens (2003) for additional motivation of this limiting non-informative specification.

$\boldsymbol{\theta} = [\theta_1 \dots \theta_n]'$ as the vector of posterior sampling weights, so that each DGP is realized as

$$g(\mathbf{z}) \mid \mathbf{Z} = \frac{1}{|\boldsymbol{\theta}|} \sum_{i=1}^n \theta_i \mathbb{1}[\mathbf{z} = \mathbf{z}_i], \quad \theta_i \stackrel{iid}{\sim} \text{Exp}(1), \quad (2)$$

where we have used the constructive definition for the Dirichlet to derive the θ_i as independent Exponentially distributed random weights with $\mathbb{E}\theta_i = 1$.

4 Representation of heterogeneous treatment effects

In order to build a rigorous concept of HTE, we adopt the Neyman/Rubin language of potential outcomes and treat our data as partially observed. Each full data point from the DGP $g(\mathbf{z})$ is then $\mathbf{z} = \{d, \mathbf{x}, \mathbf{v}\}$, where $\mathbf{v} = [v(\mathbf{c}), v(\mathbf{t})]'$ and $v(d)$ is the potential outcome either with or without treatment. Only one of these potential outcomes is actually observed: response y , corresponding to $v(\mathbf{c})$ if $d = 0$ and $v(\mathbf{t})$ if $d = 1$.

4.1 Indexing by moment conditions

Our first statistic of interest links HTE with \mathbf{x} via the vector $\boldsymbol{\gamma}$ in the moment condition, defined on the DGP in (1),

$$\mathbf{0} = \mathbb{E}_g[\mathbf{x}(v(\mathbf{t}) - v(\mathbf{c}) - \mathbf{x}'\boldsymbol{\gamma})] = \frac{1}{|\boldsymbol{\theta}|} \sum_{l=1}^L \theta_l \mathbf{x}_l (v_l(\mathbf{t}) - v_l(\mathbf{c}) - \mathbf{x}_l' \boldsymbol{\gamma}). \quad (3)$$

Thus treatment effect coefficients $\boldsymbol{\gamma}$ are the linear projection of partially observed individual treatment effects onto \mathbf{x} . They are defined such that $\mathbf{x}'\boldsymbol{\gamma}$ is uncorrelated with $v(\mathbf{t}) - v(\mathbf{c})$ in g .

Our observed data is incomplete: we only get to see one element of \mathbf{v}_i . To solve for $\boldsymbol{\gamma}$ in (3), we add an additional condition motivated by treatment randomization,

$$\mathbb{E}_g[\mathbf{x}v(d)] = \mathbb{E}_g[\mathbf{x}v(d) \mid d] = \sum_{l=1}^L \frac{\theta_l \mathbb{1}_{[d_l=d]}}{|\boldsymbol{\theta}_d|} \mathbf{x}_l v_l(d). \quad (4)$$

This says that the joint distribution of \mathbf{x} and \mathbf{v} is independent of treatment d ,⁷ which holds by

⁷Condition (4) is satisfied, say for $d = \mathbf{t}$ and with unknown $\mathbf{v}_c(\mathbf{t}) = [v_1(\mathbf{t}) \dots v_{n_c}(\mathbf{t})]'$, if $\mathbf{X}_c \text{diag}(\boldsymbol{\theta}_c) \mathbf{v}_c(\mathbf{t}) = \mathbf{X}_t \text{diag}(\boldsymbol{\theta}_t [|\boldsymbol{\theta}|/|\boldsymbol{\theta}_t| - 1]) \mathbf{y}_t$, which is an underdetermined system in $\mathbf{v}_c(\mathbf{t})$ if $p < \min(n_c, n_t)$.

construction in a fully randomized controlled trial. Conditions (3) and (4) together imply

$$\mathbb{E}_g[\mathbf{x}v(\mathbf{t})|d = 1] - \mathbb{E}_g[\mathbf{x}v(\mathbf{c})|d = 0] = \mathbb{E}_g[\mathbf{x}\mathbf{x}']\boldsymbol{\gamma}. \quad (5)$$

Define $\boldsymbol{\Theta} = \text{diag}(\boldsymbol{\theta})$ as the $n \times n$ weight operator, and similarly $\boldsymbol{\Theta}_d = \text{diag}(\boldsymbol{\theta}_d)$. The $\boldsymbol{\gamma}$ corresponding to a given realization of $\boldsymbol{\theta}$ is available as

$$\boldsymbol{\gamma} = |\boldsymbol{\theta}|(\mathbf{X}'\boldsymbol{\Theta}\mathbf{X})^{-1} \left(\frac{1}{|\boldsymbol{\theta}_t|}\mathbf{X}'_t\boldsymbol{\Theta}_t\mathbf{y}_t - \frac{1}{|\boldsymbol{\theta}_c|}\mathbf{X}'_c\boldsymbol{\Theta}_c\mathbf{y}_c \right), \quad (6)$$

where $(\mathbf{X}'\boldsymbol{\Theta}\mathbf{X})^{-1}$ denotes a Moore-Penrose pseudoinverse of the unnormalized population gram matrix.⁸ It is sometimes convenient to resolve (6) into treatment group-specific projections, in which case we write $\boldsymbol{\gamma} = \boldsymbol{\varphi}_t - \boldsymbol{\varphi}_c$ where $\boldsymbol{\varphi}_d = (|\boldsymbol{\theta}|/|\boldsymbol{\theta}_d|)(\mathbf{X}'\boldsymbol{\Theta}\mathbf{X})^{-1}\mathbf{X}'_d\boldsymbol{\Theta}_d\mathbf{y}_d$.

4.2 Differenced treatment-group OLS projections

Another common practice (e.g., Freedman, 2008; Lin, 2013) is to study HTE through the difference in ordinary least-squares (OLS) projections,

$$\mathbf{b}_t - \mathbf{b}_c = (\mathbf{X}'_t\mathbf{X}_t)^{-1}\mathbf{X}'_t\mathbf{y}_t - (\mathbf{X}'_c\mathbf{X}_c)^{-1}\mathbf{X}'_c\mathbf{y}_c. \quad (7)$$

This statistic is obviously relevant if the response is truly linear in \mathbf{x} . However, there are many applications where the difference in linear projections will be useful regardless of the true DGP. For example, Section 6 details a frequentist literature that uses (7) as a basis for semi- and non-parametric estimation of average treatment effects in the presence of heterogeneity.

From our nonparametric Bayesian perspective, the difference between treatment group *population* OLS projections is a statistic of the underlying DGP. Write the group projections as

$$\boldsymbol{\beta}_d = (\mathbf{X}'_d\boldsymbol{\Theta}_d\mathbf{X}_d)^{-1}\mathbf{X}'_d\boldsymbol{\Theta}_d\mathbf{y}_d. \quad (8)$$

This is precisely the statistic studied, using the Bayesian nonparametric model from Section 3, in Lancaster (2003) and Poirier (2011). Since the treatment groups are independent, $\boldsymbol{\beta}_t \perp\!\!\!\perp \boldsymbol{\beta}_c$

⁸It is a characteristic of this article that we are considering $p \ll n$ designs and overdetermined systems in $\boldsymbol{\gamma}$, so that this will be a standard unique inverse with very high probability.

and the posterior for the difference $\beta_t - \beta_d$ can be derived directly from the posterior on (8).

4.3 Treatment effect trees

Regression trees are a fundamental machine learning tool. They use a sequence of binary *split rules* at locations in the covariate support to partition the covariate space into regions of relatively homogeneous response. The predicted response for a given covariate location \mathbf{x} is then the average of the observed responses for observations in the same partition as \mathbf{x} .

A recent paper by Athey and Imbens (2015) applies regression trees in the measurement of heterogeneous treatment effects. For randomized controlled trials, we can take advantage of their basic algorithm that simply replaces the observed response y_i with a transformed value

$$y_i^* = y_i \frac{d_i - q}{q(1 - q)}, \quad (9)$$

where q is the probability of treatment (e.g., $q = 2/3$ in our EBay example). If treatment allocation (d_i) is considered unknown, then for a given observation i

$$\mathbb{E}[y_i^* | \mathbf{v}_i] = qv_i(\mathbf{t}) \frac{1 - q}{q(1 - q)} - (1 - q)v_i(\mathbf{c}) \frac{q}{q(1 - q)} = v_i(\mathbf{t}) - v_i(\mathbf{c}) \quad (10)$$

where the expectation here is taken simply with respect to treatment randomization. Thus a tree that is trained to fit the average value for y^* can be used to predict the treatment effect.

The CART algorithm of Breiman et al. (1984) is a common recipe for building trees; it grows greedily through a series of partitions on features, each of which maximizes reduction in some measure of impurity at the current tree leaves (terminal nodes; i.e., the implied input space partitioning). We focus on regression trees, which seek to minimize response variance within node. A given node η , containing data subset $\{\mathbf{x}_i, y_i^*\}_{i \in \eta}$, is partitioned into two child nodes according to a binary split on one of the covariate locations. For a split on input j of observation k , say $x_{kj} = x$, the two children nodes are $\text{left}(\eta, j, x) = \{i : x_{ij} \leq x\}$ and $\text{right}(\eta, j, x) = \{i : x_{ij} > x\}$. A regression CART algorithm applied to the DGP with weights

θ will choose the optimal split on η to minimize the weighted sum of squares

$$I_{\theta}^2(\eta, j, x) = \sum_{i \in \text{left}(\eta, j, x)} \theta_i (y_i^* - \mu_{\text{left}(\eta, j, x)}^*)^2 + \sum_{i \in \text{right}(\eta, j, x)} \theta_i (y_i^* - \mu_{\text{right}(\eta, j, x)}^*)^2, \quad (11)$$

where $\mu_{\text{child}(\eta, j, x)}^* = \sum_{i \in \text{right}(\eta, j, x)} y_i^* \theta_i / |\theta_{\text{right}(\eta, j, x)}|$. This splitting process repeats until the algorithm encounters a stopping rule; in this paper our trees will stop splitting when they can no longer partition into children that are larger than a specified minimum leaf size.

The impurity in (11) is a random variable. Thus each greedy split is minimizing a random function of the DGP, and the resulting CART-fit tree, say \mathcal{T}_g^* , is itself a random statistic of the unknown DGP. A posterior over \mathcal{T}_g^* is induced by our posterior on θ . To help with intuition, note that we can sample from the posterior over trees via the Bayesian bootstrap described in Section 5 below: simply draw a weight vector from the posterior and fit CART under these weights (i.e., greedily minimizing (11)). Posterior samples of CART trees built in this way are labeled a *Bayesian Forest* in Taddy et al. (2015); refer to that paper for additional detail and references on Bayesian analysis of regression trees.

4.4 Differenced treatment-group trees

A typical semi-parametric Bayesian approach to analysis of HTE specifies flexible regression functions for each of the treatment groups. The difference between posterior realizations of these group-specific functions is then interpretable as treatment heterogeneity. For example, Hill (2011) applies Bayesian additive regression trees (BART; Chipman et al., 2010) for flexible regression in each treatment group. Instead of relying upon a semi-parametric model that is likely misspecified for our data,⁹ we study separate CART tree fits for the response within each treatment group and assess their posterior under the fully nonparametric framework of Section 3. That is, we consider the same CART algorithm as in Section 4.3, but for untransformed response y and fit independently for $d = 0$ and $d = 1$ data samples. The HTE statistic of interest is then the difference between these two CART fits, say $\mathcal{T}_g^t(\mathbf{x}) - \mathcal{T}_g^c(\mathbf{x})$.

⁹For example, Hill’s BART model specifies a homogeneous Gaussian distribution for the additive error around its target surface, and would thus be inappropriate for the type of heteroskedastic errors that one expects with internet transaction data.

5 Posterior inference

The Bayesian bootstrap of Rubin (1981), outlined below in Section 5.1, is a simple algorithm for sampling from our exact posterior over arbitrary statistics. For the complex tree statistics of 4.3-4, Bayesian bootstrap sampling is our only option for posterior inference.¹⁰ For the linear projections of 4.1-2, we are also able to derive approximate posterior means and variances. Section 5.2 details these approximations, which will be useful for our theoretical understanding of the statistics of interest and for fast inference on massive datasets.

5.1 Bayesian bootstrap for posterior sampling

Consider some statistic of the DGP, say $\mathcal{S}_g \equiv \mathcal{S}(\boldsymbol{\theta})$. This could be as simple as the DGP mean, which can be written in the posterior as $\mathbf{Z}'\boldsymbol{\theta}$. For our applications, it will be one of the HTE statistics from Section 4: either a linear projection or a regression tree. Following Rubin (1981), we can obtain a sample from the posterior on γ through a simple Bayesian bootstrap.

For $b = 1, \dots, B$,

- draw $\theta_i^b \stackrel{iid}{\sim} \text{Exp}(1)$, $i = 1, \dots, n$; then
- calculate $\mathcal{S}_b = \mathcal{S}(\boldsymbol{\theta}_b)$.

The same steps can be used to obtain posterior samples for any related functionals.

5.2 Approximate posterior inference for linear projections

We proceed by studying the exact posterior on first-order Taylor series expansions for the statistic of interest around the *posterior mean DGP* solution, where $\boldsymbol{\theta} = \mathbf{1}$. Lancaster (2003) and Poirier (2011) applied this approach, under the same Bayesian nonparametric model that we use, in analysis of OLS projections. Their work applies directly to the study of our OLS-difference HTE statistic from 4.2. Since $\boldsymbol{\theta}_c \perp\!\!\!\perp \boldsymbol{\theta}_t$ (i.e., the treatment group DGPs are independent) and thus $\boldsymbol{\beta}_c \perp\!\!\!\perp \boldsymbol{\beta}_t$, we can study the difference $\boldsymbol{\beta}_t - \boldsymbol{\beta}_c$ by looking independently at each group's projection. For example, $\text{var}(\tilde{\boldsymbol{\beta}}_t - \tilde{\boldsymbol{\beta}}_c)$ has posterior variance $\text{var}(\tilde{\boldsymbol{\beta}}_t) + \text{var}(\tilde{\boldsymbol{\beta}}_c)$.

¹⁰However, in Section 8 we do reference a results from Taddy et al. (2015) on the approximate posterior for single node splits. This is the foundation for our expectation of posterior stability in the trunks of trees.

A first-order Taylor approximation to the group-specific population OLS in (8) is

$$\tilde{\beta}_d = \hat{\beta}_d + \nabla \beta_d|_{\theta_d=1}(\theta_d - 1) \quad (12)$$

where $\hat{\beta}_d = \beta_d|_{\theta_d=1} = (\mathbf{X}'_d \mathbf{X}_d)^{-1} \mathbf{X}'_d y_d$ is the OLS projection at posterior mean DGP. Following the same steps as in our Appendix 9, and as in Lancaster (2003) and Poirier (2011), the $(p+1) \times n$ gradient multiplier is available as $\nabla \beta_d = (\mathbf{X}'_d \Theta_d \mathbf{X}_d)^{-1} \mathbf{X}_d \text{diag}(y_d - \mathbf{X}_d \beta_d)$ and

$$\mathbf{G}_{\beta_d} := \nabla \beta_d|_{\theta_d=1} = (\mathbf{X}'_d \mathbf{X}_d)^{-1} \mathbf{X}_d \mathbf{R}_d \quad (13)$$

where $\mathbf{R}_d = \text{diag}(\mathbf{r}_d)$ and \mathbf{r}_d is the vector of group-specific OLS residuals, $r_i = y_i - \mathbf{x}'_i \hat{\beta}_d$ for $i \in d$. Since each θ_i has an independent exponential posterior distribution, so $\text{var}(\theta_d) = \mathbf{I}_{n_d}$, the approximation in (8) has *exact* posterior variance

$$\text{var}(\tilde{\beta}_d) := \Sigma_{\tilde{\beta}_d} = \mathbf{G}_{\beta_d} \text{var}(\theta_d) \mathbf{G}'_{\beta_d} = (\mathbf{X}'_d \mathbf{X}_d)^{-1} \mathbf{X}'_d \mathbf{R}_d \mathbf{R}_d \mathbf{X}_d (\mathbf{X}'_d \mathbf{X}_d)^{-1}. \quad (14)$$

This matches the Huber-White heteroskedastic-consistent OLS variance formula (White, 1980).¹¹

Similar steps can be applied to derive a first order approximation to our moment-condition HTE statistic from 4.1. At the posterior mean DGP, γ from (6) becomes the sample projection $\hat{\gamma} = \gamma|_{\theta=1} = n(\mathbf{X}'\mathbf{X})^{-1}(\mathbf{X}'_t \mathbf{y}_t/n_t - \mathbf{X}'_c \mathbf{y}_c/n_c)$. When necessary, we pull out each treatment group projection as $\hat{\varphi}_d = n(\mathbf{X}'\mathbf{X})^{-1} \mathbf{X}'_d \mathbf{y}_d/n_d$. Write $\nabla \mathbf{u}$ for the $\text{len}(\mathbf{u}) \times n$ derivative of a vector \mathbf{u} on θ . The first-order Taylor expansion for γ around $\theta = \mathbf{1}$ is

$$\tilde{\gamma} = \hat{\gamma} + \nabla \gamma|_{\theta=1}(\theta - \mathbf{1}). \quad (15)$$

The $(p+1) \times n$ gradient matrix, evaluated at mean $\theta = \mathbf{1}$, is derived in Appendix 9 as

$$\mathbf{G}_\gamma := \nabla \gamma|_{\theta=1} = (\mathbf{X}'\mathbf{X})^{-1} \mathbf{X}' \mathbf{E} + \left(\frac{1}{n} \hat{\gamma} \mathbf{1}' + \frac{1}{n_c} \hat{\varphi}_c \mathbf{1}'_c - \frac{1}{n_t} \hat{\varphi}_t \mathbf{1}'_t \right) \quad (16)$$

where $\mathbf{E} = \text{diag}(\mathbf{e})$ and $\mathbf{e} = [e_1 \dots e_n]'$, where $e_i = (\mathbf{1}_{[i \in t]} n_t^{-1} - \mathbf{1}_{[i \in c]} n_c^{-1}) n y_i - \mathbf{x}'_i \hat{\gamma}$ is

¹¹Lin (2013) also proposes this Huber-White variance as the basis for standard errors on interaction-adjusted average treatment effect estimates, as discussed in Section 6.

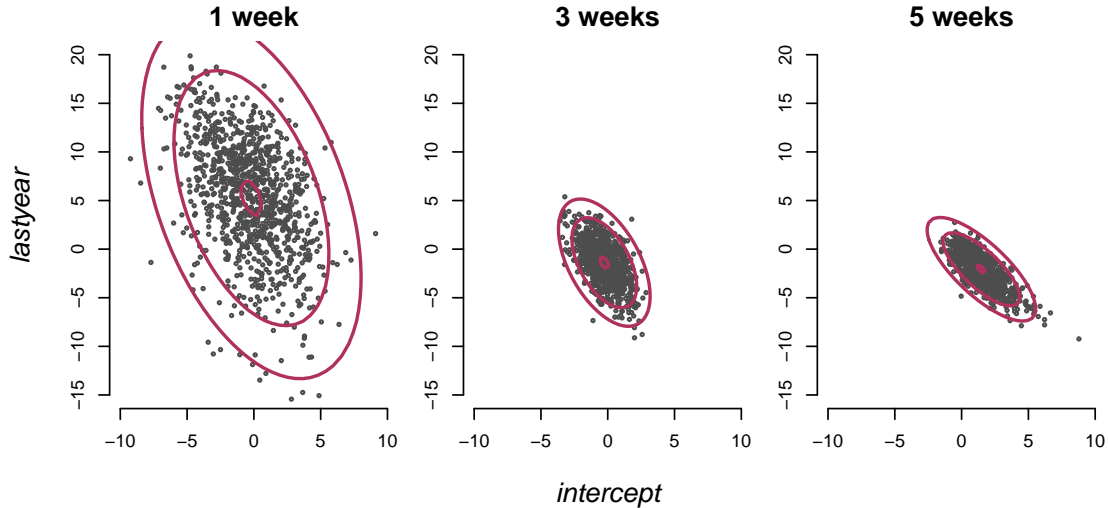


Figure 1: Posterior samples of γ_0 and γ_{lastyear} given information accumulated through 1, 3, and 5 experiment weeks. Contours correspond to a normal density centered at $\hat{\gamma}$ and with variance $\Sigma_{\tilde{\gamma}}$.

the ‘treatment effect residual’.¹² Thus $\tilde{\gamma}$ has posterior mean $\hat{\gamma}$ and exact posterior variance $\text{var}(\tilde{\gamma}) := \Sigma_{\tilde{\gamma}} = \mathbf{G}_{\gamma} \text{var}(\boldsymbol{\theta}) \mathbf{G}'_{\gamma} = \mathbf{G}_{\gamma} \mathbf{G}'_{\gamma}$. See Appendix 9 for additional detail.

5.3 Example: last-purchase-dependent heterogeneity

To aid intuition, we quickly illustrate here the relationship between the Bayesian bootstrap and its analytic approximation. Figure 1 summarizes the posterior on a length-2 γ that results from a single source of heterogeneity in our EBay experiments: whether or not the user has made at least one purchase in the past year. The intercept, γ_0 , corresponds to the treatment effect for new or lapsed users and γ_{lastyear} is the added effect for those users who made at least one purchase in the past year.¹³ We show inference conditional upon the 7.45 million users who visited their myEbay page in the first week of the experiment, the 10.97 million users who visited in the first three weeks, and the 13.22 million who visited at any time during the experiment. The posteriors are summarized through 1000 draws from the Bayesian bootstrap exact sampler and as well as through a normal distribution centered at $\hat{\gamma}$ and with variance $\Sigma_{\tilde{\gamma}}$. Notice that even after 5 weeks and 13 million exposed users, we still see evidence of posterior non-normality –

¹²Appendix 9 shows that \mathbf{e} has a mean of zero and is orthogonal to all columns of \mathbf{X} . For intuition, note that the ‘response’ implied here is almost exactly the same as the transformed response in (9): since $n_t/n \approx q$, we have that $(\mathbb{1}_{[i \in t]}/n_t - \mathbb{1}_{[i \in c]}/n_c) n y_i \approx y_i^*$. Our moment condition-derived γ is thus essentially the same indexing of heterogeneity you would get from a full-sample OLS fit for regression of the y^* values onto \mathbf{x} ; this is the linear regression analogue of the strategy advocated in Athey and Imbens (2015).

¹³Results for $\beta_t - \beta_d$ are visually very similar.

a long south-east tail – in our bootstrap samples. However, the analytic approximations appear to be doing a decent job of capturing the general location and spread of the posterior.

6 Application: Average treatment effects

Even in the presence of heterogeneity, the average treatment effect (ATE) is often of primary interest. In our Bayesian nonparametric framework, the average treatment effect is *defined* as

$$\text{ATE}_g = \mathbb{E}_g[v(\mathbf{t}) - v(\mathbf{c})] = \frac{1}{|\boldsymbol{\theta}|} \sum_l \theta_l [v_l(\mathbf{t}) - v_l(\mathbf{c})]. \quad (17)$$

Like any other posterior functional, ATE_g is a random variable. Since each \mathbf{v} is only partially observed, (17) is useless without more information about the unobserved potential outcomes. However, each of the HTE statistics in Section 4 implies its own variant of ATE_g based upon its indexing of the treatment effects on covariates; this section will study these ATE statistics.

6.1 ATE statistics that are not adjusted by covariates

Recall the moment condition in (4), $\mathbb{E}_g[\mathbf{x}v(\mathbf{d})] = \mathbb{E}_g[\mathbf{x}v(\mathbf{d})|d]$, which is justified by treatment randomization and is necessary to solve for $\boldsymbol{\gamma}$ from Section 4.1. Since \mathbf{x} always includes an intercept, the first dimension of (4) implies that $\mathbb{E}_g v(\mathbf{d}) = \mathbb{E}_g[v(\mathbf{d})|d]$, so that

$$\text{ATE}_g^{\text{obs}} := \frac{1}{|\boldsymbol{\theta}_t|} \boldsymbol{\theta}'_t \mathbf{y}_t - \frac{1}{|\boldsymbol{\theta}_c|} \boldsymbol{\theta}'_c \mathbf{y}_c = \mathbb{E}_g[v(\mathbf{t})|d=1] - \mathbb{E}_g[v(\mathbf{c})|d=0] = \text{ATE}_g. \quad (18)$$

Thus (4) restricts ATE_g to be the difference between *observable* treatment and control averages for a given DGP, a random variable which we denote $\text{ATE}_g^{\text{obs}}$. It is easy to see $\text{ATE}_g^{\text{obs}}$ has posterior mean equal to $\bar{y}_t - \bar{y}_c$. Since $\text{var}(\mathbf{v}'\boldsymbol{\theta}/|\boldsymbol{\theta}|) = \mathbf{v}'\text{cov}(\boldsymbol{\theta}/|\boldsymbol{\theta}|)\mathbf{v} = \frac{1}{n(n+1)} \mathbf{v}' [\mathbf{I} - \frac{1}{n}] \mathbf{v} = \frac{1}{n+1} [\frac{1}{n} \mathbf{v}'\mathbf{v} - \bar{v}^2]$ and weights conditional upon each treatment status are independent from each other, it has exact posterior variance available as

$$\text{var}(\text{ATE}_g^{\text{obs}}) = \text{var}(\mathbf{y}'_t \boldsymbol{\theta}_t / |\boldsymbol{\theta}_t|) + \text{var}(\mathbf{y}'_c \boldsymbol{\theta}_c / |\boldsymbol{\theta}_c|) = \frac{1}{n_t(n_t + 1)} s_{\mathbf{y}_t}^2 + \frac{1}{n_c(n_c + 1)} s_{\mathbf{y}_c}^2. \quad (19)$$

where $s_v^2 = \mathbf{v}'\mathbf{v} - n_v \bar{v}^2$ is the sum-squared-error for generic length- n_v vector \mathbf{v} . This is a slight deflation of the usual frequentist sample variance formula.

The sources of heterogeneity contained in \mathbf{x} play no role in (18).¹⁴ This occurs because the mechanism whereby we were able to index partially observed treatment effects onto covariates – the moment restriction of (4) – implies a value for ATE_g . A similar situation arises for the treatment effect trees of Section 7.3, which effectively replace $v_i(\mathbf{t}) - v_i(\mathbf{c})$ with the transformed response, $y^* = y_i(d_i - q) / [q(1 - q)]$. This implies the ATE statistic

$$\text{ATE}_g^* := \frac{1}{|\boldsymbol{\theta}|} \boldsymbol{\theta}' \mathbf{y}^*, \quad (20)$$

with exact posterior mean \bar{y}^* and variance $\text{var}(\text{ATE}_g^*) = s_{\mathbf{y}^*}^2 / [n(n + 1)]$. Again, the covariates have no influence: ATE_g^* is the average predicted treatment effect for *any* realization of our CART tree from Section 4.3.

6.2 Regression adjusted ATE statistics

In contrast to the examples above, where covariates play no role in the ATE statistic, there is a large frequentist literature on the use of covariates to improve estimation for average treatment effects. In these studies, the statistician provides a ‘regression adjusted’ estimator for various definitions of a *true* ATE (see Imbens, 2004, for a survey of frequentist inferential targets). The advantage of such estimators is that they can have lower sampling variance than the simple difference in treatment group means. When the regression adjustment introduces little or no bias, it leads to more efficient estimation.

Recall \mathbf{b}_d as the treatment group OLS projections from (7). If $\mathbf{x}'_i \mathbf{b}_d$ is expected to be near $v_i(d)$, then a regression adjusted estimator for the average treatment effect is

$$\widehat{\text{ATE}} = \bar{\mathbf{x}}'(\mathbf{b}_t - \mathbf{b}_c). \quad (21)$$

More precisely, $\widehat{\text{ATE}}$ is an estimator for the *sample average treatment effect*, $\sum_{i=1}^n v_i(\mathbf{t}) - v_i(\mathbf{c})$, or for the *population average treatment effect*, $\mathbb{E}_f[v_i(\mathbf{t}) - v_i(\mathbf{c})]$ with \mathbb{E}_f here denoting the

¹⁴Indeed, say $\boldsymbol{\mu} = \mathbf{X}'\boldsymbol{\theta}/|\boldsymbol{\theta}|$; because γ is derived directly from the restriction in (4), it is easy to show that $\boldsymbol{\mu}'\boldsymbol{\gamma} = \text{ATE}_g^{\text{obs}}$. A direct corollary is that at the posterior mean DGP, with $\boldsymbol{\theta} = \mathbf{1}$, we have $\bar{\mathbf{x}}'\hat{\boldsymbol{\gamma}} = \bar{y}_t - \bar{y}_c$.

frequentist’s expectation under a true but unknown data generating process f .

One way to justify (21) is to assume a linear relationship between \mathbf{x} and $v_i(d)$. Linearity holds trivially if there are a small number of discrete (or discretized) covariates and \mathbf{x} represents a partitioning of the data into constant-level subsets. Application of (21) in this situation is referred to as *post stratification*; see Deng et al. (2013) for use in context of digital experiments and Miratrix et al. (2013) for a detailed theoretical overview. Use of \widehat{ATE} can also be justified for situations where linearity does not hold. Berk et al. (2013), Pitkin et al. (2013), Lin (2013), and Lin (2014) study ATE estimation under a variety of assumed sampling models. In each case, they show that \widehat{ATE} is an asymptotically more efficient estimator of average treatment effects than the simple difference in means, $\bar{y}_t - \bar{y}_c$. Crucially, this advantage holds even if the relationships between \mathbf{x} and the $v(d)$ are nonlinear.¹⁵

The analogous nonparametric Bayesian procedure would consider covariate averages projected through our difference in population OLS lines from (8), leading to the linearly-adjusted

$$ATE_g^{\text{lin}} = \boldsymbol{\mu}'(\boldsymbol{\beta}_t - \boldsymbol{\beta}_c) = \frac{1}{|\boldsymbol{\theta}|} \boldsymbol{\theta}' \mathbf{X} \left((\mathbf{X}'_t \boldsymbol{\Theta}_t \mathbf{X}_t)^{-1} \mathbf{X}'_t \boldsymbol{\Theta}_t \mathbf{y}_t - (\mathbf{X}'_c \boldsymbol{\Theta}_c \mathbf{X}_c)^{-1} \mathbf{X}'_c \boldsymbol{\Theta}_c \mathbf{y}_c \right). \quad (22)$$

As always, this is a random variable. In agreement with the frequentist literature, we find in Appendix B that a first-order approximation to ATE_g^{lin} does indeed tend to have a lower posterior variance than ATE_g^{obs} . Theorem B.1 shows

$$\text{var} (ATE_g^{\text{lin}}) \approx \text{var}(ATE_g^{\text{obs}}) - \left(\frac{R_t^2 s_{y_c}^2}{n_t^2} + \frac{R_c^2 s_{y_c}^2}{n_c^2} \right), \quad (23)$$

where $R_d^2 = 1 - s_{r_d}^2 / s_{y_d}^2$ is the coefficient of determination (proportion of deviance explained) for the group d OLS regression. Thus regression adjustment yields a large variance reduction only if elements of \mathbf{x} have large covariances with y and if the sample size is not too big.¹⁶

Linear regression adjustment is often applied in the presence of nonlinearity and, perhaps more importantly, omitted covariate interactions. Although the frequentist arguments cited above show that such adjustment can be helpful despite misspecification, an alternative ap-

¹⁵See also Tsiatis et al. (2008), Moore et al. (2011), Tian et al. (2012), and Yuan et al. (2012) for regression adjustment strategies that include selection on covariates.

¹⁶In our specific EBay experiment, Bayesian bootstrap samples from the exact posterior find little evidence of any drop in posterior variance for ATE_g^{lin} vs ATE_g^{obs} . See Section 6.3 for detail.

proach would be to replace the linear projections with more flexible regression techniques. This is the argument made convincingly in the semi- and non-parametric regression literature, e.g., Hill (2011), Grimmer et al. (2013), Imai and Ratkovic (2013), and references therein. Our Bayesian nonparametric version of this approach would be to consider the average predicted treatment effect obtained by differencing the treatment-group specific trees of Section 4.4,

$$\text{ATE}_g^{\text{tree}} = \frac{1}{|\boldsymbol{\theta}|} \sum_i \theta_i [\mathcal{T}_g^{\text{t}}(\mathbf{x}_i) - \mathcal{T}_g^{\text{c}}(\mathbf{x}_i)]. \quad (24)$$

We can apply the Bayesian bootstrap to obtain a posterior distribution over $\text{ATE}_g^{\text{tree}}$, yielding flexible regression adjustment with a fully nonparametric accounting of posterior uncertainty.

Posterior Mean (and SD)

	week 1	week 2	week 3	week 4	week 5
$\text{ATE}_g^{\text{obs}}$	3.30 (2.04)	1.34 (1.24)	1.44 (0.95)	1.71 (0.80)	1.90 (0.76)
ATE_g^*	3.84 (1.22)	1.65 (0.84)	1.70 (0.69)	1.96 (0.61)	2.09 (0.60)
$\text{ATE}_g^{\text{lin}}$	2.95 (2.07)	1.26 (1.29)	1.39 (0.84)	1.55 (0.72)	1.83 (0.75)
$\bar{\mathbf{x}}(\tilde{\beta}_{\text{t}} - \tilde{\beta}_{\text{c}})$	3.05 (2.04)	1.15 (1.24)	1.29 (0.95)	1.59 (0.80)	1.80 (0.76)
$\text{ATE}_g^{\text{tree}}$	2.99 (1.46)	1.03 (1.46)	1.20 (0.90)	1.74 (0.80)	1.75 (0.82)
number of users, in mil	7.45	9.48	10.97	12.20	13.22

Table 1: Inference on ATE statistics for users who visited their myEbay page through 1-5 weeks, cumulative. Values for $\text{ATE}_g^{\text{obs}} = \mathbf{y}'_{\text{t}}\boldsymbol{\theta}_{\text{t}}/|\boldsymbol{\theta}_{\text{t}}| - \mathbf{y}'_{\text{c}}\boldsymbol{\theta}_{\text{c}}/|\boldsymbol{\theta}_{\text{c}}|$, $\text{ATE}_g^* = \boldsymbol{\theta}'\mathbf{y}^*/|\boldsymbol{\theta}|$, and $\bar{\mathbf{x}}(\tilde{\beta}_{\text{t}} - \tilde{\beta}_{\text{c}})$ are exact posterior means and standard deviations, while $\text{ATE}_g^{\text{lin}} = \boldsymbol{\mu}'(\beta_{\text{t}} - \beta_{\text{c}})$ and $\text{ATE}_g^{\text{tree}} = \sum_i \theta_i [\mathcal{T}_g^{\text{t}}(\mathbf{x}_i) - \mathcal{T}_g^{\text{c}}(\mathbf{x}_i)] / |\boldsymbol{\theta}|$ moments are based upon 100 draws from the Bayesian bootstrap.

6.3 EBay illustration: average treatment effects

We illustrate posterior inference for average treatment effects using the EBay spending data from Section 2, including the full covariate set from Section 2.2. Posterior means and standard deviations, calculated for users who had visited their myEBay page by the end of each week, are in Table 1. Posterior means for the five ATE statistics – one based on each of our four HTE statistics, plus a linear approximation to $\text{ATE}_g^{\text{lin}}$ – are all within a fraction of their standard deviation from each other at any point in time. The standard deviations for observed differences

ATE_g^{obs} are very close to those for the OLS-adjusted ATE_g^{lin} , its approximation $\bar{x}(\tilde{\beta}_t - \tilde{\beta}_c)$, and the tree-adjusted ATE_g^{tree} ,¹⁷ such that there is little or no variance reduction benefit here from *any* regression adjustment. From (23), we guess that this occurs because the sample sizes are very large and the response is only weakly correlated with x . In contrast, the mean of the transformed treatment-effect response, $ATE_g^* = \theta' y^* / |\theta|$, does have a 15-25% lower posterior standard deviation here than the other statistics. Since $\text{var}(ATE_g^*)$ shrinks with total n while $\text{var}(ATE_g^{obs})$ shrinks with the group-specific n_d , this can occur whenever the sample variance for y^* is not much larger than the within-group sample variances for y_d .

7 Application: Sparse summarization of linear HTE projections

Understanding of the heterogeneity in treatment effects is a key ingredient in decision making about those treatments. The linear HTE statistics from Sections 4.1-2, including the moment condition solution γ and the difference in OLS lines $\beta_t - \beta_c$, provide an interpretable indexing of such heterogeneity: each coordinate represents the expected change in $v(t) - v(c)$ per unit increase in the corresponding covariate. The methods of Section 5 allow for a nonparametric accounting of the uncertainty about these relationships, e.g., as plotted in Figure 1.

The full p -variable story told by γ or by $\beta_t - \beta_c$ is often too high dimensional to be useful for decision makers. Moreover, the coordinates of these projections can have high uncertainty and are correlated with each other in their posterior. In such settings, it is useful to project down from these full vectors to a small set of relationships that summarize the HTE information.

7.1 A sparse decision rule

Suppose that you have the $p + 1$ dimensional posterior over some HTE projection, say τ for either γ or $\beta_t - \beta_c$. The task at hand is to come up with a sparse approximation of τ which summarizes this full posterior distribution. This is a decision problem, and it can be addressed through Bayesian decision theory as detailed in, e.g., Berger (1985). The action space consists of vectors δ that approximate τ , and our *loss function* must penalize both discrepancy between γ and δ and the number of nonzero elements in δ .

¹⁷The tree is fit under the same settings as in Section 8, with minimum leaf size of $1e^5$ and maximum depth of 5.

Hahn and Carvalho (2014) review sparse posterior summarization in the context of prediction problems. They argue that, for many problems, the discrepancy between posterior realizations for the parameter of interest and its sparse summary should be measured in terms of predictive fit. A similar argument applies to our situation, where we wish to penalize the distance between fitted HTE representations, $\mathbf{X}\boldsymbol{\tau}$, and its sparse approximation, $\mathbf{X}\boldsymbol{\delta}$. Applying L_2 loss on this distance and adding a cost for the size of the support of $\boldsymbol{\delta}$, yields our loss function

$$L(\boldsymbol{\delta}) = \sum_i v_i (\mathbf{x}'_i \boldsymbol{\delta} - \mathbf{x}'_i \boldsymbol{\tau})^2 + 2n\lambda \|\boldsymbol{\delta}\|_0, \quad (25)$$

where λ is the ‘cost of complexity’ and $v_i > 0$ is an observation-specific weight on the approximation loss. We consider both $v_i = 1$, as in Hahn and Carvalho, and $v_i = 1/\text{var}(\mathbf{x}'_i \boldsymbol{\tau})$, the posterior precision (or its approximation) for the treatment-effect projection of user i .

The posterior expected loss is then, with $P(\boldsymbol{\tau})$ the posterior distribution,

$$\begin{aligned} \int L(\boldsymbol{\delta}) dP(\boldsymbol{\tau}) &= \sum_i \int v_i \left[(\mathbf{x}'_i \boldsymbol{\tau})^2 - 2\mathbf{x}'_i \boldsymbol{\tau} \mathbf{x}'_i \boldsymbol{\delta} + (\mathbf{x}'_i \boldsymbol{\delta})^2 \right] dP(\boldsymbol{\tau}) + 2n\lambda \|\boldsymbol{\delta}\|_0 \\ &= \sum_i v_i \left[\text{var}(\mathbf{x}'_i \boldsymbol{\tau}) + (\mathbf{x}'_i \mathbb{E}[\boldsymbol{\tau}])^2 - 2\mathbf{x}'_i \mathbb{E}[\boldsymbol{\tau}] \mathbf{x}'_i \boldsymbol{\delta} + (\mathbf{x}'_i \boldsymbol{\delta})^2 \right] + 2n\lambda \|\boldsymbol{\delta}\|_0 \\ &= \sum_i v_i (\mathbf{x}'_i \boldsymbol{\delta} - \mathbf{x}'_i \mathbb{E}[\boldsymbol{\tau}])^2 + 2n\lambda \|\boldsymbol{\delta}\|_0 + \sum_i v_i \text{var}(\mathbf{x}'_i \boldsymbol{\tau}). \end{aligned} \quad (26)$$

In practice, we will replace $\mathbb{E}[\boldsymbol{\tau}]$ with its value at the posterior mean DGP where $\boldsymbol{\theta} = \mathbf{1}$, say $\hat{\boldsymbol{\tau}}$. Removing constants then yields the posterior expected loss objective

$$R(\boldsymbol{\delta}) = \sum_i v_i (\mathbf{x}'_i \boldsymbol{\delta} - \mathbf{x}'_i \hat{\boldsymbol{\tau}})^2 + 2n\lambda \|\boldsymbol{\delta}\|_0. \quad (27)$$

For precision weighting, we again rely upon the approximate moments of Section 5.2 and set $v_i = 1/\mathbf{x}'_i \Sigma_{\hat{\boldsymbol{\tau}}} \mathbf{x}_i \approx 1/\text{var}(\mathbf{x}'_i \boldsymbol{\tau})$, where $\Sigma_{\hat{\boldsymbol{\tau}}}$ is the approximate variance (either $\Sigma_{\hat{\boldsymbol{\tau}}}$ or $\Sigma_{\hat{\beta}_t} + \Sigma_{\hat{\beta}_c}$).

7.2 Approximate L_0 penalized minimization

The L_0 -penalized objective in (27) is nearly impossible to optimize for \mathbf{x}_i with more than a few non-independent variables. A common strategy replaces the L_0 cost with a more tractable

L_1 -penalty (i.e., the lasso of Tibshirani, 1996). Weighted L_1 penalties that replace $\|\delta\|_0$ with $\sum_j w_j |\delta_j|$, where weights $w_j \geq 0$ are data-dependent, can be used to get even closer to the L_0 ideal. For example, the adaptive lasso of Zou (2006) uses weights proportional to the inverse of a guess for the optimal solution, say $w_j = 1/|\hat{\delta}_j|$, while Fan et al. (2014) sets w_j through 1-2 steps of an iterative solver targeting a concave penalized function. Taddy (2014) surveys a variety of such weighted L_1 approximations to L_0 penalties and advocates weights that adapt along a regularization path. Objectives as in (27) are solved for a decreasing grid of $\lambda_1 > \lambda_2 \cdots > \lambda_T$, where $\|\delta\|_0$ at grid-point t is replaced by $\sum_j w_j^t |\delta_j|$ and w_j^t is $1/|\delta_j^{t-1}|$, the inverse of the solution at $t - 1$.¹⁸ We will apply this algorithm via the `gamlr` R package from Taddy (2014), which is fast to run and very memory efficient for sparse covariate designs.

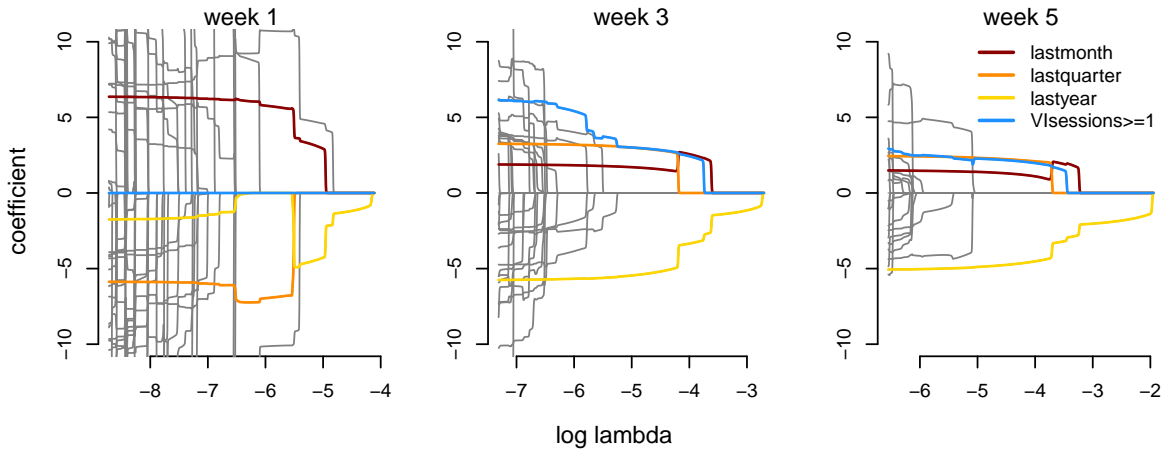


Figure 2: Paths for approximate minimization of the posterior expected loss in (27) as a function of complexity cost when targeting γ and with weights $v_i = 1/\mathbf{x}'_i \Sigma_{\gamma} \mathbf{x}_i$. The panels show the sparse approximation to γ under the posterior distribution after one, three, and five weeks of the experiment.

7.3 EBay illustration: sparse linear posterior summarization

Consider γ and $\beta_t - \beta_c$ from Section 4.1-2. These are length-378 vectors for the linear design described in Section 2.2, and a full posterior is available for each. This is far too much information to communicate to managers and executives, so we need to focus on a small number of key dimensions. Using the procedure detailed above, each vector can be summarized with a sparse δ : the decision rule which minimizes our posterior expected loss in (27). For example, Figure 2 shows the length-1000 grid for δ as a function of complexity cost, λ_t , that is obtained

¹⁸All weights start at $w_j^t = 1$, and λ_1 is the largest value such that $\delta_j^1 = 0$ for all j .

by (approximately, as in Section 7.2) minimizing the posterior expected loss for (27). This figure is for target functional γ and with loss weights $v_i = 1/\mathbf{x}_i' \Sigma_{\gamma} \mathbf{x}_i$. Each point along the paths presents a possible sparse summarization, depending upon one’s tolerance for complexity. As data accumulates throughout the experiment, the coefficients in our sparse summary settle down and stabilize. In week one, many coefficients take absolute values > 10 and are off-the-chart, while by week five they have settled down to lie mostly between ± 5 .

Table 2 shows the 5-dimensional summaries that result from minimizing the posterior expected loss in (27), both unweighted ($v_i = 1$) and weighted by the posterior precision for the first-order approximation to τ . Imagining path plots like those in Figure 2 for each of our target/weight combinations, these summaries are located at the leftmost (smallest λ_t) vertical slice that cuts only 4 nonzero lines (the intercept is not plotted). The summary for τ under precision-weighted loss is the fastest to stabilize. By week 3 we have converged to the same summary as in week 5: positive coefficients for *lastmonth* and *lastquarter*, a negative effect for *lastyear*, and a positive effect for $VI_{sessions} \geq 1$ – an indicator for whether the user had clicked on an item to see its ‘view item’ page at least once in the four weeks prior to the experiment. Note that the negative *lastyear* coefficient essentially cancels out the intercept, so that the effect of increasing the image size on user spend tends to be more positive for either new users or for those who have been active in the past quarter or month. In addition, the effect was larger for those users who have previously felt the need to view an item in detail.

Under precision-weighted loss, the summaries for target $\beta_t - \beta_c$ are similar to those for γ . In contrast, minimization of unweighted expected loss yields sparse projections that differ much more from each other across both weeks and targets. If you desire that the summaries should stabilize as we accumulate data (or be stable between choice of target), then the precision-weighted loss is giving preferable results in this example. The unweighted loss minimization is chasing values of $\mathbf{x}_i' \tau$ that have large expectation but high variance – e.g., corresponding to \mathbf{x}_i locations at the edge of our support. Although it may seem strange to have posterior variance as part of one’s loss function, this appears to be essential for getting reliable results when uncertainty is hugely variable across observations.

target (τ)	weights (v_i)	week	variables (and coefficient) in the sparse approximation
γ	$1/\mathbf{x}'_i \Sigma_{\gamma} \mathbf{x}_i$	1	<i>lastmonth</i> (5.78), <i>lastquarter</i> (-6.96), <i>Vviews</i> ≥ 1 (10.73), <i>Vviews</i> ≥ 13 (-10.14)
		2	<i>lastmonth</i> (5.62), <i>lastyear</i> (-7.26), <i>Vviews</i> ≥ 1 (7.9), <i>Vviews</i> ≥ 13 (-3.96)
		3	<i>lastmonth</i> (1.74), <i>lastquarter</i> (3.05), <i>lastyear</i> (-5.53), <i>Vsessions</i> ≥ 1 (3.05)
		4	<i>lastmonth</i> (2.05), <i>lastquarter</i> (3.31), <i>lastyear</i> (-5.28), <i>Vsessions</i> ≥ 1 (2.15)
		5	<i>lastmonth</i> (1.39), <i>lastquarter</i> (2.32), <i>lastyear</i> (-4.89), <i>Vsessions</i> ≥ 1 (2.27)
γ	1	1	<i>lastmonth</i> (3.77), <i>SRPviews</i> ≥ 1 (4.86), <i>SRPviews</i> ≥ 254 (12.93), <i>SRPsessions</i> ≥ 10 (-14.95)
		2	<i>lastmonth</i> (5.04), <i>BI</i> ≥ 12 (8.39), <i>SpendElectronics</i> ≥ 22.9 (-12.9), <i>Vviews</i> ≥ 1 (6.48)
		3	<i>lastquarter</i> (3.38), <i>BidsOther</i> ≥ 7 (0.71), <i>SRPviews</i> ≥ 254 (1.83), <i>Vsessions</i> ≥ 1 (3.29)
		4	<i>lastquarter</i> (3.35), <i>BI</i> ≥ 12 (4.49), <i>myEBaySessions</i> ≥ 12 (-3.06), <i>Vsessions</i> ≥ 1 (2.86)
		5	<i>lastmonth</i> (1.73), <i>BI</i> ≥ 12 (8.29), <i>SpendBIN</i> ≥ 232.8 (-5.01), <i>SRPsessions</i> ≥ 2 (2.34)
$\beta_t - \beta_c$	$1/\mathbf{x}'_i (\Sigma_{\beta_t} + \Sigma_{\beta_c}) \mathbf{x}_i$	1	<i>lastmonth</i> (5.4), <i>lastquarter</i> (-6.81), <i>SRPviews</i> ≥ 1 (9.08), <i>Vviews</i> ≥ 13 (-8.33)
		2	<i>lastmonth</i> (5.07), <i>lastyear</i> (-6.82), <i>Vviews</i> ≥ 1 (7.1), <i>Vviews</i> ≥ 13 (-3.35)
		3	<i>lastmonth</i> (1.3), <i>lastquarter</i> (2.88), <i>lastyear</i> (-5.04), <i>Vviews</i> ≥ 1 (2.7)
		4	<i>lastmonth</i> (1.55), <i>lastquarter</i> (3.18), <i>lastyear</i> (-4.74), <i>Vviews</i> ≥ 1 (1.66)
		5	<i>lastmonth</i> (0.94), <i>lastquarter</i> (2.3), <i>lastyear</i> (-4.45), <i>SRPsessions</i> ≥ 2 (2.4)
$\beta_t - \beta_c$	1	1	<i>SRPviews</i> ≥ 1 (4.82), <i>SRPviews</i> ≥ 254 (10.2), <i>SRPsessions</i> ≥ 10 (-17.58), <i>WI</i> ≥ 11 (11.49)
		2	<i>lastmonth</i> (4.29), <i>BI</i> ≥ 12 (8.61), <i>SpendElectronics</i> ≥ 22.9 (-13.01), <i>Vviews</i> ≥ 1 (5.99)
		3	<i>lastquarter</i> (2.82), <i>Bids</i> ≥ 2 (-3.12), <i>BidsOther</i> ≥ 7 (36.42), <i>Vsessions</i> ≥ 1 (3.65)
		4	<i>lastquarter</i> (2.97), <i>BI</i> ≥ 6 (3.57), <i>myEBaySessions</i> ≥ 12 (-3.58), <i>SRPsessions</i> ≥ 2 (2.38)
		5	<i>lastquarter</i> (1.25), <i>AskSellerQuestion</i> ≥ 1 (-2.3), <i>BI</i> ≥ 12 (8.3), <i>SpendBIN</i> ≥ 232.8 (-4.06)

Table 2: Five-dimensional sparse summaries of the linear HTE projections from Sections 4.1-2, obtained by approximately minimizing the posterior expected loss in (27) using the `gam1r` package in R. For each of linear projection we consider both unweighted loss and that weighted by an approximation to the posterior precision, $1/\text{var}(\mathbf{x}'_i \tau)$. We show the four non-intercept variables and their coefficients in the resulting sparse summary. These values correspond to the minimum λ_t at which $\|\delta\|_0 = 4$. Terminology includes: *views* is the count of page impressions, *sessions* is the number of sessions where an event occurs, *SRP* is a search results page, *VI* is where the user clicked on a item to view details, *BI* is the count of bought items, *BIN* is the ‘buy-it-now’ (fixed-price) platform, *Bids* are bids on the auction platform, and *WI* is the number of items a user has added to their watch-list.

8 Stable trees and partitioning

Our final application will consider the partitioning of users, along covariate values, into groups wherein we predict relatively homogeneous response to treatment.¹⁹ We will study a statistic that implies such partitioning directly: the treatment effect trees of Athey and Imbens (2015), as outlined in Section 4.3, which apply the CART tree algorithm on transformed response, y^* .

If one wishes to predict the treatment effect for future users, the usual strategy would be to obtain the posterior *mean* for some useful prediction rule. In our case, the predicted treatment response for user i with covariates \mathbf{x}_i would be the average of the predictions from each tree in a Bayesian forest – the posterior sample of CART regression trees obtained through Bayesian bootstrap sampling. This strategy, detailed in Taddy et al. (2015), is closely related to the popular and successful Random forest algorithm (Breiman, 2001). Thus, instead of the cross-validated pruning of a *single* tree described in Athey and Imbens (2015), both standard Bayesian procedure and a large bank of experience in machine learning would advocate for *averaging* predictions across many un-pruned trees.

However, Athey and Imbens (2015) limit themselves to a single tree because they want not only to predict, but also to do so through an interpretable prediction rule. Forests lose the appealing simplicity and interpretability of a tree: there is no longer a single hierarchy of splits, and there is no longer a single implied data partitioning. In particular, if you wish to design separate treatments (e.g., products) for different groups of users, then you can do so for each leaf node of a single tree. A forest of possible trees is of little help in such a scenario.

If you need a single tree, the sample CART fit is an obvious choice. However, trees are only trustworthy down to a certain depth, after which they become over-fit (hence the pruning in Athey and Imbens). Fortunately, we can use our Bayesian nonparametric framework to assess the confidence that we should have in different portions of the sample CART tree structure. Taddy et al. (2015) studied the posterior for the optimal split location on a single tree node under the DGP model from Section 3. They find that the variance of this split location is low for large samples, such that the tops of trees (where the nodes contain much of the data) will be

¹⁹Such partitioning could also be addressed through the sparse linear methods above in Section 7: for example, our precision-weighted 5-Dimensional summary of γ could be applied to split users into 8 groups according to the value of their last-purchase indicators (month/quarter/year) and whether the user visited a view-item page.

stable on massive datasets. Thus there is hope that with enough data we can find partitioning rules that are included in an optimal CART with high posterior probability.

8.1 EBay illustration: posterior uncertainty for tree structure

Consider the two regression trees in Figure 3, fit after one and after five weeks of experimentation. The trees have been grown greedily from top to bottom²⁰, as described in Section 4.3, and the leaf nodes are marked with the corresponding expected treatment effect: $\mathbb{E}[y_i^* \mid i \in \eta] = \mathbb{E}[v_i(\mathbf{t}) - v_i(\mathbf{c}) \mid i \in \eta]$. For the variables included in each tree, Table 3 contains the posterior probability that the variable is split upon at or above a given depth in the CART fit for a new realization of the DGP. In the Week 1 tree, fit to 7.45 million users, only *Bids Fashion* – the number of bids on items in the ‘fashion’ category – occurs with greater than 1/3 probability at a depth ≤ 5 . However, after observing 5 weeks of purchasing from 13.22 million users, there are five variables that occur in more than 1/3 of depth-5 trees. Moreover, three variables occur with probability greater than 1/2: *SI Fashion*, the number of sold fashion items; *Bids Other*, the number of bids on un-categorized items; and the *lastmonth* indicator. The split locations within the variables are also stable: a range of 14-17 for *SI Fashion* and 7-10 for *Bids Other*. Thus we can partition users into four groups according to the splits implied by these three variables and have a better than 1/2 chance²¹ that for any posterior DGP realization a similar partitioning will be included in the top of the optimal regression tree.

9 Conclusion

This article describes a complete Bayesian nonparametric framework for quantifying uncertainty when connecting heterogeneous treatment effects to covariates in a randomized controlled trial. We’ve analyzed an array of HTE statistics – linear and tree-based, both for synthetic response and fit separately within each treatment group – in a wide ranging survey of applications and in the context of our EBay example. This serves to illustrate the Bayesian nonparametric model and its application, as well as to provide a case study of the issues relevant to treatment effect estimation from A/B experiments in a large technology company.

²⁰We fit all of our trees in distribution using MLLIB’s decision tree methods in Apache Spark

²¹See Barbieri and Berger (2004) for discussion of median probability Bayesian variable selection.

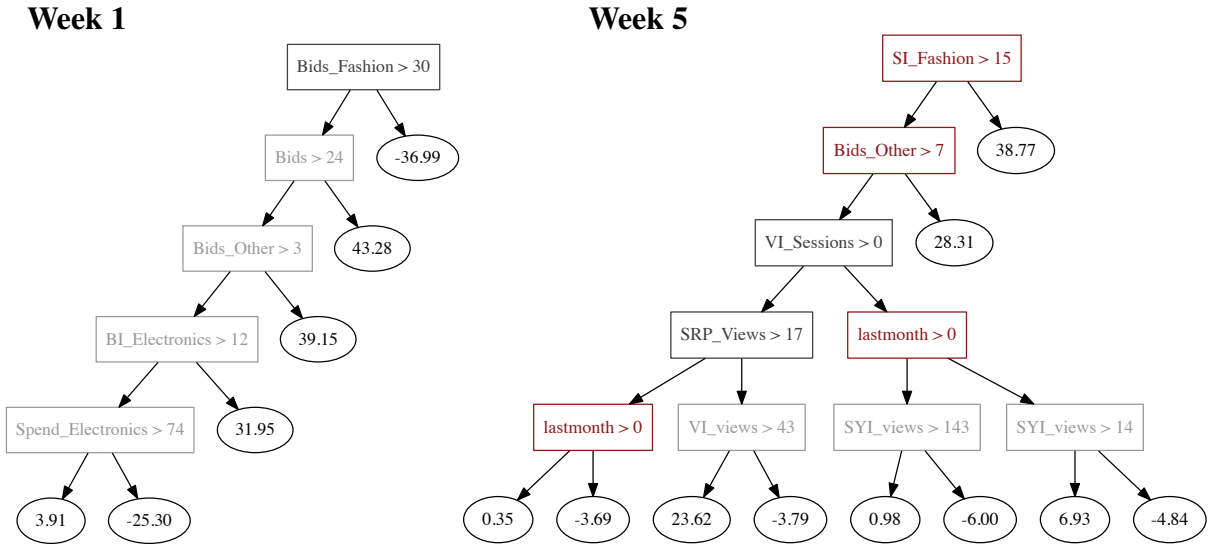


Figure 3: Sample CART trees after one and five weeks of experimentation. The algorithm was run with a minimum leaf size of 100,000 users and a maximum depth of 5 internal (splitting) nodes. The right children contain data for which the split condition is true, and left children are the complement. The leaf nodes are marked with the expected response in that leaf. Decision nodes are colored according to the posterior probability that the corresponding variable is included in the CART fit for new a DGP realization: light grey for $p < \frac{1}{3}$, dark grey for $p \in [\frac{1}{3}, \frac{1}{2})$, and red for $p \geq \frac{1}{2}$. Most of the variables are defined in the caption for Table 2; in addition, *SI* denotes the count of items sold by the user and *SYI* denotes the count of items that the user attempted to sell through the ‘sell your item’ interface.

Variable split probabilities		Week 5				
		depth in tree				
Week 1	depth in tree					
	1	≤ 2	≤ 3	≤ 4	≤ 5	
<i>BidsFashion</i>	.25	.30	.35	.35	.35	
<i>Bids</i>	.00	.05	.15	.20	.30	
<i>Bids Other</i>	.10	.20	.25	.25	.25	
<i>BI Electronics</i>	.05	.15	.15	.25	.25	
<i>Spend Electronics</i>	.05	.15	.15	.15	.20	
<i>SI Fashion</i>	.45	.50	.50	.50	.50	
<i>Bids Other</i>	.30	.75	.75	.75	.75	
<i>VI sessions</i>	.05	.05	.05	.10	.35	
<i>lastmonth</i>	.05	.10	.15	.40	.65	
<i>SRP views</i>	.00	.10	.15	.25	.40	
<i>VI views</i>	.00	.00	.10	.20	.25	
<i>SYI views</i>	.00	.00	.05	.15	.25	

Table 3: Posterior probabilities of CART splitting at or above depths 1 to 5 on each of the variables in the corresponding sample CART tree, after each of one and five weeks of experimentation. These probabilities are obtained from Bayesian bootstrap samples (i.e., a Bayesian forest) of size 20 for CART run under the same settings as our sample tree: maximum depth of 5 and minimum leaf size of 100,000.

We do not advocate this Bayesian nonparametric framework as the only approach to inference. There are obviously important frequentist considerations that go into choosing one HTE statistic over another in any application. A Bayesian semi-parametric analysis could yield more efficient estimation even if some of the model assumptions are not strictly correct. There are conceptual issues with the $a \rightarrow 0$ limiting prior specification in our multinomial sampling model specification: it should be thought of as a theoretical construct that we hope does a good job of representing finite sample uncertainty. This should hold for the massive samples encountered in digital experiments, but such bootstrap-related methods will break down in larger p settings (especially with a fat-tailed response) and we should not be overconfident.

However, all that aside, the classic Bayesian nonparametric setup of Section 3 provides a useful fresh perspective on uncertainty about HTE. Approximate posterior moments for the linear models allow us to compare Bayesian and frequentist nonparametric uncertainty quantification, and they allow for more stable sparse summaries through a precision-weighted loss function. The ability to sample from the exact posterior via the Bayesian bootstrap is also hugely useful: in this way we are able to quantify uncertainty about structure in the CART trees that are increasingly a popular method for HTE prediction. In each case, we hope that our different perspective might add something to the current view of these HTE analyses.

Appendices

A Details for approximate posterior inference

A.1 Gradient

Say $\omega = \frac{1}{|\theta|}\theta$ and $\Omega = \text{diag}(\omega)$, and similarly for Ω_d . Define $\mathbf{S} = \mathbf{X}'\Omega\mathbf{X}$. Then

$$\nabla\varphi_d = (\mathbf{S}^{-1}\mathbf{y}_d \otimes \mathbf{X}'_d)\nabla\text{vec}(\Omega_d) - (\mathbf{y}'_d\Omega_d\mathbf{X}_d \otimes \mathbf{I}_{p+1})(\mathbf{S}^{-1} \otimes \mathbf{S}^{-1})(\mathbf{X}' \otimes \mathbf{X}')\nabla\text{vec}(\Omega) \quad (28)$$

$$= \mathbf{y}'_d \otimes \mathbf{S}^{-1}\mathbf{X}'_d\nabla\text{vec}(\Omega_d) - \mathbf{y}'_d\Omega_d\mathbf{X}_d\mathbf{S}^{-1}\mathbf{X}' \otimes \mathbf{S}^{-1}\mathbf{X}'\nabla\text{vec}(\Omega)$$

$$= \mathbf{y}'_d \otimes \mathbf{S}^{-1}\mathbf{X}'_d\nabla\text{vec}(\Omega_d) - \varphi'_d\mathbf{X}' \otimes \mathbf{S}^{-1}\mathbf{X}'\nabla\text{vec}(\Omega). \quad (29)$$

This simplifies considerably upon noting that

$$\nabla \text{vec}(\boldsymbol{\Omega}) = \begin{bmatrix} \frac{\partial \omega_1}{\partial \boldsymbol{\theta}} & \mathbf{0}_{n \times n} & \frac{\partial \omega_2}{\partial \boldsymbol{\theta}} & \mathbf{0}_{n \times n} & \cdots & \mathbf{0}_{n \times n} & \frac{\partial \omega_n}{\partial \boldsymbol{\theta}} \end{bmatrix}', \quad (30)$$

where $\partial \omega_i / \partial \boldsymbol{\theta}$ is the length- n vector with j^{th} element $\mathbb{1}_{[i=j]} / |\boldsymbol{\theta}| - \theta_j / |\boldsymbol{\theta}|^2$, and similarly for $\nabla \text{vec}(\boldsymbol{\Omega}_d)$ but with rows missing and columns zero for $j \notin d$. Thus, for example,

$$\nabla \boldsymbol{\varphi}_c = \frac{1}{|\boldsymbol{\theta}_c|} \left[(\mathbf{S}^{-1} \mathbf{X}'_c \text{diag}(\mathbf{y}_c) - \boldsymbol{\varphi}_c \mathbf{1}'_{n_c}) \mathbf{0}'_{n_t} \right] - \frac{1}{|\boldsymbol{\theta}|} (\mathbf{S}^{-1} \mathbf{X}' \text{diag}(\mathbf{X} \boldsymbol{\varphi}_c) - \boldsymbol{\varphi}_c \mathbf{1}'_n) \quad (31)$$

is the $(p+1) \times n$ gradient matrix for the control group projection. Taking $\nabla \boldsymbol{\gamma} = \nabla \boldsymbol{\varphi}_t - \nabla \boldsymbol{\varphi}_c$ and evaluating at $\bar{\boldsymbol{\theta}} = \mathbf{1}$, where $\mathbf{S} = \mathbf{X}' \mathbf{X} / n$ and $\boldsymbol{\varphi}_d = \hat{\boldsymbol{\varphi}}_d$, we arrive at the expression in (16).

A.2 Treatment effect residuals

We also consider the residuals defined in Section 5.2 as $e_i = \left(\frac{\mathbb{1}_{[i \in t]}}{n_t} - \frac{\mathbb{1}_{[i \in c]}}{n_c} \right) n y_i - \mathbf{x}'_i \hat{\boldsymbol{\gamma}}$.

PROPOSITION A.1. Write $\mathbf{e}_c = [e_1, \dots, e_{n_c}]$, $\mathbf{e}_t = [e_{n_c+1}, \dots, e_n]'$, and $\mathbf{e} = \begin{bmatrix} \mathbf{e}_c \\ \mathbf{e}_t \end{bmatrix}$. Then

$$(i) \quad \mathbf{1}' \mathbf{e} = \mathbf{0} \quad (ii) \quad -\mathbf{X}'_c \mathbf{e}_c = \mathbf{X}'_t \mathbf{e}_t = \mathbf{X}'_t \mathbf{X}_t \hat{\boldsymbol{\varphi}}_c + \mathbf{X}'_c \mathbf{X}_c \hat{\boldsymbol{\varphi}}_t \quad (iii) \quad \mathbf{X}' \mathbf{e} = \mathbf{0}.$$

Proof. For i , we use $\bar{\mathbf{y}}_t - \bar{\mathbf{y}}_t = \bar{\mathbf{x}}' \hat{\boldsymbol{\gamma}}$. For ii , notice that

$$\mathbf{X}_c = -\frac{n}{n_c} \mathbf{X}'_c \mathbf{y}_c - \mathbf{X}'_c \mathbf{X}_c (\mathbf{X}' \mathbf{X})^{-1} \left[\frac{n}{n_c} \mathbf{X}'_t \mathbf{y}_t - \frac{n}{n_c} \mathbf{X}'_c \mathbf{y}_c \right].$$

Multiplying the first term by $\mathbf{I} = (\mathbf{X}'_c \mathbf{X}_c + \mathbf{X}'_t \mathbf{X}_t) (\mathbf{X}' \mathbf{X})^{-1}$ and collecting terms gives our result. Finally, iii is a direct consequence of ii . \square

A.3 Variance calculations

For computation, one can use results from above to expand the variance $\Sigma_{\bar{\boldsymbol{\gamma}}} = \mathbf{G}_\gamma \mathbf{G}'_\gamma$ as

$$\Sigma_{\bar{\boldsymbol{\gamma}}} = (\mathbf{X}' \mathbf{X})^{-1} \mathbf{X}' \mathbf{E} \mathbf{E} \mathbf{X} (\mathbf{X}' \mathbf{X})^{-1} + \mathbf{B} + \mathbf{B}' + \left(\frac{1}{n_c} \hat{\boldsymbol{\varphi}}_c \hat{\boldsymbol{\varphi}}'_c + \frac{1}{n_t} \hat{\boldsymbol{\varphi}}_t \hat{\boldsymbol{\varphi}}'_t - \frac{1}{n} \hat{\boldsymbol{\gamma}} \hat{\boldsymbol{\gamma}}' \right) \quad (32)$$

$$\begin{aligned}
\text{with } \mathbf{B} &= (\mathbf{X}'\mathbf{X})^{-1} \left[\mathbf{X}'_c \mathbf{e}_c \left(\frac{1}{n} \hat{\gamma} + \frac{1}{n_c} \hat{\varphi}_c \right)' + \mathbf{X}'_t \mathbf{e}_t \left(\frac{1}{n} \hat{\gamma} - \frac{1}{n_t} \hat{\varphi}_t \right)' \right] \\
&= -(\mathbf{X}'\mathbf{X})^{-1} \left[(\mathbf{X}'_t \mathbf{X}_t \hat{\varphi}_c + \mathbf{X}'_c \mathbf{X}_c \hat{\varphi}_t) \left(\frac{1}{n_c} \hat{\varphi}_c + \frac{1}{n_t} \hat{\varphi}_t \right)' \right]. \tag{33}
\end{aligned}$$

B Posterior inference for regression adjustment

An approximation to $\text{ATE}_g^{\text{lin}} = \boldsymbol{\mu}'(\beta_t - \beta_c)$ is $\bar{\mathbf{x}}'(\tilde{\beta}_t - \tilde{\beta}_c)$, with variance $\bar{\mathbf{x}}'(\Sigma_{\tilde{\beta}_t} + \Sigma_{\tilde{\beta}_c})\bar{\mathbf{x}}$.

THEOREM B.1.

$$\begin{aligned}
\text{var} \left(\bar{\mathbf{x}}' [\tilde{\beta}_t - \tilde{\beta}_c] \right) &= \frac{s_{y_c}^2}{n_t^2} + \frac{s_{y_c}^2}{n_c^2} - \left(\frac{R_t^2 s_{y_c}^2}{n_t^2} + \frac{R_c^2 s_{y_c}^2}{n_c^2} \right) \\
&\quad + (\bar{\mathbf{x}} - \bar{\mathbf{x}}_t)' \Sigma_{\tilde{\beta}_t} (\bar{\mathbf{x}} - \bar{\mathbf{x}}_t) + (\bar{\mathbf{x}} - \bar{\mathbf{x}}_c)' \Sigma_{\tilde{\beta}_c} (\bar{\mathbf{x}} - \bar{\mathbf{x}}_c), \tag{34}
\end{aligned}$$

where $s_v^2 = \mathbf{v}'\mathbf{v} - n_v \bar{v}^2$ for generic length- n_v vector \mathbf{v} and $R_d^2 = 1 - s_{r_d}^2/s_{y_d}^2$.

Proof. Consider the shifted OLS projections $\dot{\beta}_d = (\dot{\mathbf{X}}_d' \Theta_d \dot{\mathbf{X}}_d)^{-1} \dot{\mathbf{X}}_d' \Theta_d \mathbf{y}_d$, using design $\dot{\mathbf{X}}_d$ that has been centered within each group so that $\dot{\mathbf{X}}_d' \boldsymbol{\theta}_d = \begin{bmatrix} n_d \\ 0_p \end{bmatrix}$. Say $\tilde{\beta}_d$ is the first order approximation of (12) applied to $\dot{\beta}_d$, with variance $\text{var}(\tilde{\beta}_d) = (\dot{\mathbf{X}}_d' \dot{\mathbf{X}}_d)^{-1} \dot{\mathbf{X}}_d' \mathbf{R}_d \mathbf{R}_d \dot{\mathbf{X}}_d (\dot{\mathbf{X}}_d' \dot{\mathbf{X}}_d)^{-1}$. Note that the residuals \mathbf{r}_d are unchanged and that the non-intercept coefficients are exactly equal: $\tilde{\beta}_{dj} = \dot{\beta}_{dj}$ for $j > 0$. Thus $\bar{\mathbf{x}}' \tilde{\beta}_d = \tilde{\beta}_{d0} + [\bar{\mathbf{x}} - \bar{\mathbf{x}}_d]' \tilde{\beta}_d = \tilde{\beta}_{d0} + [\bar{\mathbf{x}} - \bar{\mathbf{x}}_d]' \dot{\beta}_d$ with variance $\text{var}(\tilde{\beta}_{d0} + [\bar{\mathbf{x}} - \bar{\mathbf{x}}_d]' \tilde{\beta}_d) = \frac{1}{n_d^2} \mathbf{r}_d' \mathbf{r}_d + (\bar{\mathbf{x}} - \bar{\mathbf{x}}_d)' \Sigma_{\tilde{\beta}_d} (\bar{\mathbf{x}} - \bar{\mathbf{x}}_d)$. Using $\mathbf{r}_d' \mathbf{r}_d = (1 - R_d^2) s_{y_d}^2$ and summing $\text{var}(\bar{\mathbf{x}}' \tilde{\beta}_t) + \text{var}(\bar{\mathbf{x}}' \tilde{\beta}_c)$ completes the result. \square

Making the rough equivalence $n_d \approx n_d + 1$ to match with $\text{var}(\text{ATE}_g)$ in (19) and stating $\bar{\mathbf{x}} - \bar{\mathbf{x}}_c \approx \mathbf{0}$ since all \mathbf{x}_i are drawn from the same distribution leads to our expression in (23).

Note that the formula in (34) ignores variance in $\text{ATE}_g^{\text{lin}}$ due to uncertainty about the covariate mean, $\boldsymbol{\mu} = \mathbf{X}'\boldsymbol{\omega}$, which is correlated with $\tilde{\beta}_t - \tilde{\beta}_c$ and has variance

$$\Sigma_{\boldsymbol{\mu}} = \mathbf{X}' \text{cov}(\boldsymbol{\omega}) \mathbf{X} = \frac{1}{n(n+1)} \mathbf{X}' \left[\mathbf{I} - \frac{1}{n} \right] \mathbf{X} = \frac{1}{n+1} \left[\frac{1}{n} \mathbf{X}'\mathbf{X} - \bar{\mathbf{x}}\bar{\mathbf{x}}' \right]. \tag{35}$$

Thus the full variance of a regression adjusted treatment effect average based upon our first-order approximation is $\text{var} \left(\boldsymbol{\mu}' [\tilde{\beta}_t - \tilde{\beta}_c] \right) > \text{var} \left(\bar{\mathbf{x}}' [\tilde{\beta}_t - \tilde{\beta}_c] \right)$, a small inflation of (34).

References

- Athey, S. and Imbens, G. (2015), “Machine Learning Methods for Estimating Heterogeneous Causal Effects,” *arXiv: 1504.01132*.
- Barbieri, M. M. and Berger, J. O. (2004), “Optimal predictive model selection,” *Annals of Statistics*, 870–897.
- Berger, J. O. (1985), *Statistical decision theory and Bayesian analysis*, Springer.
- Berk, R., Pitkin, E., Brown, L., Buja, A., George, E., and Zhao, L. (2013), “Covariance Adjustments for the Analysis of Randomized Field Experiments,” *Evaluation Review*, 37, 170–196.
- Breiman, L. (2001), “Random forests,” *Machine Learning*, 45, 5–32.
- Breiman, L., Friedman, J., Olshen, R., and Stone, C. (1984), *Classification and regression trees*, Chapman & Hall/CRC.
- Chamberlain, G. and Imbens, G. W. (2003), “Nonparametric Applications of Bayesian Inference,” *Journal of Business & Economic Statistics*, 21, 12–18.
- Chipman, H. A., George, E. I., and McCulloch, R. E. (2010), “BART: Bayesian Additive Regression Trees,” *The Annals of Applied Statistics*, 4, 266–298.
- Deng, A., Xu, Y., Kohavi, R., and Walker, T. (2013), “Improving the sensitivity of online controlled experiments by utilizing pre-experiment data,” in *Proceedings of the sixth ACM international conference on Web search and data mining*, ACM, pp. 123–132.
- Duan, N., Manning, W. G., Morris, C. N., and Newhouse, J. P. (1983), “A comparison of alternative models for the demand for medical care,” *Journal of Business & Economic Statistics*, 1, 115.
- Fan, J., Xue, L., and Zou, H. (2014), “Strong oracle optimality of folded concave penalized estimation,” *The Annals of Statistics*, 42, 819–849.
- Ferguson, T. (1973), “A Bayesian analysis of some nonparametric problems,” *Annals of Statistics*, 1, 209–230.
- Freedman, D. A. (2008), “On regression adjustments to experimental data,” *Advances in Applied Mathematics*, 40, 180–193.
- Grimmer, J., Messing, S., and Westwood, S. J. (2013), “Estimating Heterogeneous Treatment Effects and the Effects of Heterogeneous Treatments with Ensemble Methods,” .
- Hahn, R. and Carvalho, C. (2014), “Decoupling shrinkage and selection in Bayesian linear models: a posterior summary perspective,” Tech. rep.
- Hill, J. L. (2011), “Bayesian Nonparametric Modeling for Causal Inference,” *Journal of Computational and Graphical Statistics*, 20, 217–240.
- Imai, K. and Ratkovic, M. (2013), “Estimating Treatment Effect Heterogeneity in Randomized Program Evaluation,” *The Annals of Applied Statistics*, 7, 443–470.

- Imbens, G. (2004), “Nonparametric Estimation Of Average Treatment Effects under Exogeneity: A Review,” *The Review of Economics and Statistics*, 86, 4–29.
- Lancaster, T. (2003), “A note on bootstraps and robustness,” Tech. rep., Working Paper, Brown University, Department of Economics.
- Lin, W. (2013), “Agnostic notes on regression adjustments to experimental data: Reexamining Freedmans critique,” *The Annals of Applied Statistics*, 7, 295–318.
- (2014), “Comments on Covariance adjustments for the analysis of randomized field experiments,” *Evaluation Review*, 38, 449–451.
- Miratrix, L. W., Sekhon, J. S., and Yu, B. (2013), “Adjusting treatment effect estimates by post-stratification in randomized experiments,” *Journal of the Royal Statistical Society: Series B (Statistical Methodology)*, 75, 369–396.
- Moore, K. L., Neugebauer, R., Valappil, T., and van der Laan, M. J. (2011), “Robust extraction of covariate information to improve estimation efficiency in randomized trials,” *Statistics in Medicine*, 30, 2389–2408.
- Pitkin, E., Berk, R., Brown, L., Buja, A., George, E., Zhang, K., and Zhao, L. (2013), “Improved precision in estimating average treatment effects,” *arXiv preprint arXiv:1311.0291*.
- Poirier, D. J. (2011), “Bayesian Interpretations of Heteroskedastic Consistent Covariance Estimators Using the Informed Bayesian Bootstrap,” *Econometric Reviews*, 30, 457–468.
- Rubin, D. (1981), “The Bayesian bootstrap,” *The Annals of Statistics*, 9, 130–134.
- Scott, S. L. (2010), “A modern Bayesian look at the multi-armed bandit,” *Applied Stochastic Models in Business and Industry*, 26, 639–658.
- Taddy, M. (2014), “One-step estimator paths for concave regularization,” arXiv:1308.5623.
- Taddy, M., Chen, C.-S., Yu, J., and Wyle, M. (2015), “Bayesian and Empirical Bayesian Forests,” in *Proceedings of the 32nd International Conference on Machine Learning (ICML 2015)*.
- Tian, L., Cai, T., Zhao, L., and Wei, L.-J. (2012), “On the covariate-adjusted estimation for an overall treatment difference with data from a randomized comparative clinical trial,” *Biostatistics*, 13, 256–273.
- Tibshirani, R. (1996), “Regression shrinkage and selection via the lasso,” *Journal of the Royal Statistical Society, Series B*, 58, 267–288.
- Tsiatis, A. A., Davidian, M., Zhang, M., and Lu, X. (2008), “Covariate adjustment for two-sample treatment comparisons in randomized clinical trials: A principled yet flexible approach,” *Statistics in Medicine*, 27, 4658–4677.
- White, H. (1980), “A heteroskedasticity-consistent covariance matrix estimator and a direct test for heteroskedasticity,” *Econometrica*, 48, 817.
- Yuan, S., Zhang, H. H., and Davidian, M. (2012), “Variable selection for covariate-adjusted semiparametric inference in randomized clinical trials,” *Statistics in Medicine*, 31, 3789–3804.
- Zou, H. (2006), “The Adaptive Lasso and Its Oracle Properties,” *Journal of the American Statistical Association*, 101, 1418–1429.